Journal of Magnetics 8(1), 24-31 (2003)

Properties and Applications of Magnetic Tunnel Junctions

G. Reiss*, H. Brückl, A. Thomas, M. Justus, D. Meyners and H. Koop

University of Bielefeld, Department of Physics, Universitätsstrasse 25, 33619 Bielefeld, Germany

(Received 10 December 2002)

The discoveries of antiferromagnetic coupling in Fe/Cr multilayers by Grünberg, the Giant Magneto Resistance by Fert and Grünberg and a large tunneling magnetoresistance at room temperature by Moodera have triggered enormous research on magnetic thin films and magnetoelectronic devices. Large opportunities are especially opened by the spin dependent tunneling resistance, where a strong dependence of the tunneling current on an external magnetic field can be found. We will briefly address important basic properties of these junctions like thermal, magnetic and dielectric stability and discuss scaling issues down to junction sizes below 0.01 μm² with respect to single domain behavior, switching properties and edge coupling effects. The second part will give an overview on applications beyond the use of the tunneling elements as storage cells in MRAMs. This concerns mainly field programmable logic circuits, where we demonstrate the clocked operation of a programmed AND gate. The second 'unconventional' feature is the use as sensing elements in DNA or protein biochips, where molecules marked magnetically with commercial beads can be detected *via* the dipole stray field in a highly sensitive and relatively simple way.

Key words : tunnel junction, magnetoresistance, biological molecules, biochips

1. Introduction

The discovery of antiferromagnetic coupling (AFC) in metallic Fe/Cr multilayers by Peter Grünberg [1] has triggered enormous research activities in the area of magnetic thin films. Such metallic layer systems additionally show the Giant Magneto Resistance (GMR), *i.e.* a very strong dependence of the resistance on an external magnetic field.

Additional opportunities are opened by a similar effect occurring in magnetic tunnel junctions (MTJ's) [2, 3] consisting of, *e.g.*, two different ferromagnetic electrodes separated by a thin insulator (Al_2O_3 in most cases). Here, the tunneling probability depends on the relative orientation of the magnetizations of the electrodes and thus a large dependence of the tunneling current on an external magnetic field can be found. This effect is usually called Tunneling Magneto Resistance (TMR) and can again be used both for detecting external fields as well as for information storage.

Much more possible applications are still ahead, especially after the finding of magnetoelectronic effects in semiconductors and the possibility to construct field programmable all magnetic logic devices. In this contribution, we will discuss some basic physical properties of these systems with special regard to their applicability and give examples for current and future applications.

*Corresponding author: Tel: +49-521-106-5411 (Secr.: -5412, Fax: -6046), e-mail: reiss@physik.uni-bielefeld.de

2. TMR effect

If two ferromagnetic metals F1 and F2 are separated by a non-ferromagnetic spacer layer, the transport of electrons will depend on the relative orientation of the magnetization in the ferromagnets due to the exchange splitting of the conduction bands. The spacer layer can be either a metal enabling electron transport between the magnetic films or an insulator thin enough for significant electron tunneling.

Electrons traveling from F1 to F2 will find different densities of states due to the exchange splitting of the bands in the ferromagnets. In the ideal case of complete spin polarization of the electrons at the fermi level, transport across the spacer would be therefore completely suppressed in the case of antiparallel magnetizations and infinitely large TMR-values could be observed. In reality, however, this spin polarization is usually restricted to values around 50% resulting in corresponding lower TMR

values.

Major challenges in the preparation of such tunneling elements are

- Keeping the roughness small enough, so that smooth tunneling barriers can be obtained down to thicknesses smaller than 1nm
- Ensuring a truly antiparallel alignment of the magnetizations of the two ferromagnetic electrodes for field ranges meeting the demands of applications
- Increasing the magnetic, dielectric and thermal stability of the tunneling elements
- Preparing and characterizing tunneling junctions with lateral sizes down to smaller than 200 nm
- Introducing a rotational like magnetic switching behavior by means of induced anisotropy and appropriate field pulses
- Increasing the TMR by changing the barrier and electrode materials.

Here, we will briefly review some of the more recent improvements and then concentrate on some 'unconventional' possible applications of these devices.

3. Tunneling Junctions

We deal with magnetic tunnel junctions, *i.e.* the potential of the spacer layer creates of a tunneling barrier. Such MTJ's have gained considerable interest due to their potential as magnetic memory cells (MRAM), as read heads in hard disc drives [4-8] or other applications [9, 10].

Within a short time, major breakthroughs concerning these demands could be obtained in the last years. This can be best illustrated by comparing results from 1999 and from 2002 (Fig. 1). In Fig. 1a, the minor and major loop of a tunneling junction biased only by an artificially antiferromagnetic Co/Cu/Co trilayers with a TMR lower than 20% and not reproducible minor loop is shown. Fig. 1b gives the example for a junction biased by the combination of antiferromagnetic IrMn with a CoFe/Ru/CoFe trilayers. Using such layer systems, TMR values between 45% and larger than 50% combined with reproducible switching behavior can now been routinely obtained.

In Fig. 2, we show a transmission electron microscopy image of a cross section of an MTJ. As can be seen, the insulating barrier can be deposited homogeneously and smooth and can even withstand annealing experiments. Thus these junctions offer the potential to be integrated in conventional micropatterning processes.

The description of the tunneling process including the exchange splitting of the bands in the ferromagnets, the partial spin polarization of the electrons close to the fermi level and the different contributions of d-like and s-like electrons to the tunneling current seems to be not yet completely solved. There are, however, approaches which give reasonable insight in the basic physics of the

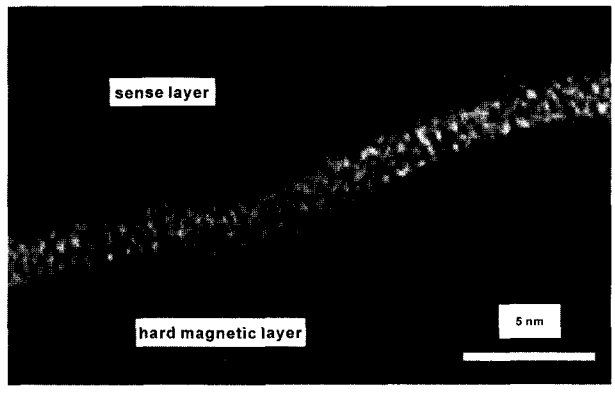

Fig. 2. Transmission electron microscopy of a cross section of a tunneling element after annealing at 400 °C. There are no hints for a damage of the barrier.

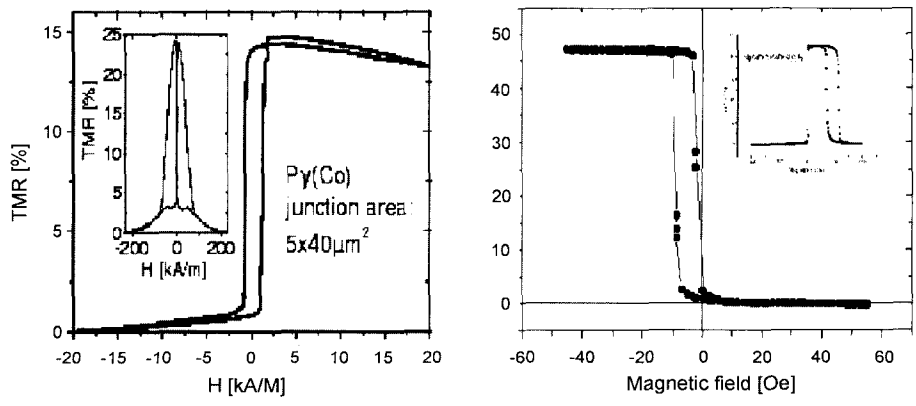

Fig. 1. Resistance as a function of an external magnetic field (minor loops) for a tunneling junction Co/Cu/Co/Al_2O_3/$Ni_{80}Fe_{20}$ (a, 1999) and IrMn/CoFe/Ru/CoFe/Al_2O_3/$Ni_{80}Fe_{20}$ (b, 2002). The TMR increased from about 15% to 45% (the insets show the corresponding major loops).

tunneling process. Most of these introduce a spin dependent tunneling probability $T_{\sigma\sigma'}$ in order to take into account the exchange splitted band structure of the electrodes.For $T_{\sigma\sigma'}$, Bratkowsky obtained [11]:

$$T_\sigma = \sum_{\sigma'} T_{\sigma\sigma'}$$

$$T_{\sigma\sigma'} = \frac{16 m_1 m_3 m_2^2 k_{1\sigma} k_{3\sigma} \kappa^2}{(m_2^2 k_{1\sigma}^2 + m_1^2 \kappa^2)(m_2^2 k_{3\sigma}^2 + m_3^2 \kappa^2)} \bullet e^{-2\kappa d} \qquad (1)$$

with σ indicating the spins at the two sides of the barrier, index 1 and 2 the left and right ferromagnet, respectively and m_3 and κ the electronic properties inside the barrier.

Eq. (1) shows, that the tunneling current will depend on the orientations of the spins in the ferromagnets. Additionally, however, the variation of the current upon changing the magnetizations, *i.e.* the TMR, will depend on the applied bias voltage, because this causes a shift of the exchange splitted band structure. This makes the situation somewhat more complicated than in GMR elements.

Although, however, TMR values of almost 60% have been reported [12], long-term application of MTJs requires properties like temperature- [6-8] or magnetic switching stability [13]. The temperature stability obtained now ranges up to around 350 °C an still needs to be improved by optimizing the materials. Due to the large knowledge about diffusion barriers obtained in the semiconductor research, this issue seems to be not a major obstacle.

Magnetic stability means a stable magnetization state of the hard layer during minor loop cycling. Some groups investigated the magnetization state of hard electrodes, consisting of hard magnets (*e.g.* $Co_{75}Pt_{12}Cr_{13}$ [13, 14]) or exchange-biased layers (*e.g.* FeMn/Co [13] or IrMn/CoFe/Ru/CoFe as in our case). Usually, an unaffected magnetization of the hard magnets by rotating field cycles is found in contrast with an instability if the soft layers are switched unidirectional. In the exchange-biased system the magnetization can be stable even after switching cycles [13]. As discussed in [15], the instability of the magnetization in the hard layer induced by cycling the soft layer originates from the large fringing fields of the magnetic domain walls of the soft layer. In an MRAM chip, however, switching will be performed by using two field pulses, one in the hard, the other one in the easy axis direction. This method induces a rotational like switching and thus magnetic stability seem to be possible at least far above the superparamagnetic size limit.

Fig. 1b already showed the dependence of the resistance of an MTJ as a function of an external magnetic field. The 'major loop' displayed in the inset gives the overall behavior of the resistance, *i.e.* the field was large enough to saturate both electrodes. For applications, the 'minor loops' (Fig. 1b) at small fields, *i.e.* where only the magnetically soft electrode is switched by the external field are important. These 'minor loops' should show two distinct states of the resistance of the element at zero field which can be attributed to parallel and antiparallel magnetization of the soft electrode with respect to the hard one. This behavior can be used for storing one bit and therefore offers the possibility to employ MTJ's in magnetic storage devices. The example of Fig. 1b, although having a large TMR value and distinct and stable magnetic states, is thus not an ideal curve for these applications due to only one resistance state at zero field. In the following, we will discuss reasons for this behavior and show improvements obtained recently.

3.1. Experimental–Tunneling cells

The magnetically hard electrode of the MTJs discussed here consists of a simple artificial antiferromagnet (AAF) Co/Cu/Co or CoFe/Ru/CoFe exchange biased by IrMn [8, 16]. The layer stacks are deposited in a dc magnetron sputtering system with a base pressure of 5×10^{-8} mbar on the native oxide of Si(100) wafers. The soft bilayers have no intentionally induced magnetic anisotropy. The TMR defined as $(\Delta R)/R_s$ is measured by two- and four-probe DC technique. The MTJs have an area resistance defined as $A^*(\Delta R)/2$ of about 50 $k\Omega\mu m^2$ and a minor loop TMR signal between 45% and 53% for the exchange biased systems at room temperature. The switching fields of the soft bilayers are ≤ 2 kA/m. The soft layer is ferromagnetically coupled with the hard electrode due to orange peel interaction [17], resulting in a hysteresis shift of 0.3 kA/m. The patterning was done by conventional e-beam lithography with subsequent Ar ion etching down to junction sizes of around 40 nm.

Many of the basic demands of MRAM like temperature stability, magnetic and dielectric stability seem to be met already. Thus we will concentrate on the scalability of the TMR effect in ultrasmall elements, which is closely related to the magnetic behavior in small dimensions.

Scalability

A question of major importance is the scalability of the TMR effect. Cell sizes around 200 nm are anticipated for the first MRAM-generations and much smaller cells will be needed in the following years.

In Fig 3, we show simulations (OOMMF code, http://math.nist.gov/oommf) and magnetic force microscopy images of small elliptic TMR cells obtained after switching in the remanent state [18]. Fig. 3a gives the magnetization in the saturated state; Fig. 3b is the magnetization

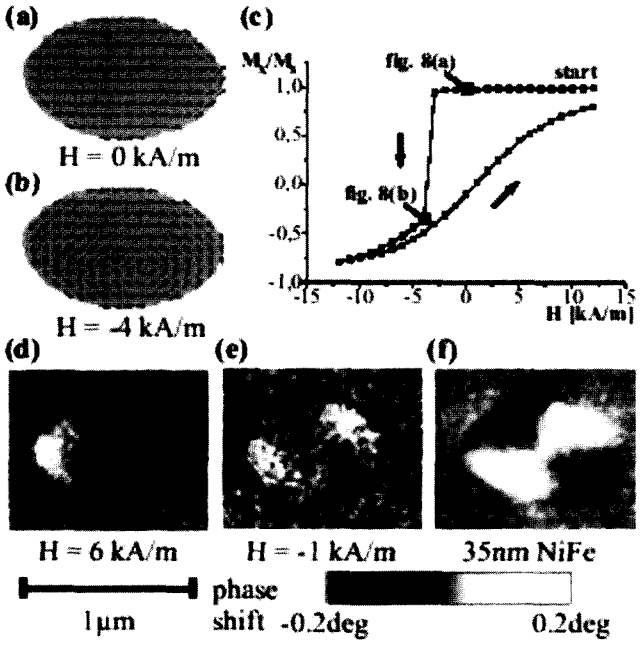

Fig. 3. Simulation of the magnetization of an elliptic element in the saturated state (a), after minor loop cycling (b), the corresponding hysteresis loop (c) and MFM images (d, e) (the cell in f has a thicker Py layer in order to enhance the magnetic stray field).

after minor loop cycling. As can be seen, a magnetic vortex was created which gives rise to the resulting asymmetric magnetization loop in Fig. 3c. Fig.'s 3d and e show the corresponding MFM images of a tunneling cell (note that the cell in Fig. 3f has a thicker $Ni_{80}Fe_{20}$ (Permalloy, Py) layer in order to enhance the magnetic contrast). Here, the measurements and the simulations show very good agreement: Elliptic cells frequently show vortex states after minor loop cycling, whereas rectangular ones often have 360° domain walls leading also to magnetization loops which are not suitable for memory cells.

In order to investigate even smaller cells, we customized another Atomic Force Microscope with the possibility to detect the tunneling current through a junction by contacting it with a conducting diamond tip [19]. Here, we are additionally able to measure complete asteroid-curves using a double pair of Helmholtz coils.

Fig. 4 shows first examples of TMR minor loops detected with this system. In Fig. 4a, the element size was 100 nm × 300 nm, in Fig. 4b 50 nm × 50 nm. The smaller junction is the smallest we were able to characterize up to now. As can be seen, the larger rectangular junction shows steps in the minor loop pointing to the switching of domains. Additionally, the resistance is not saturated after the closure of the hysteresis, which could be related with non parallel biasing and easy axis directions. In contrast

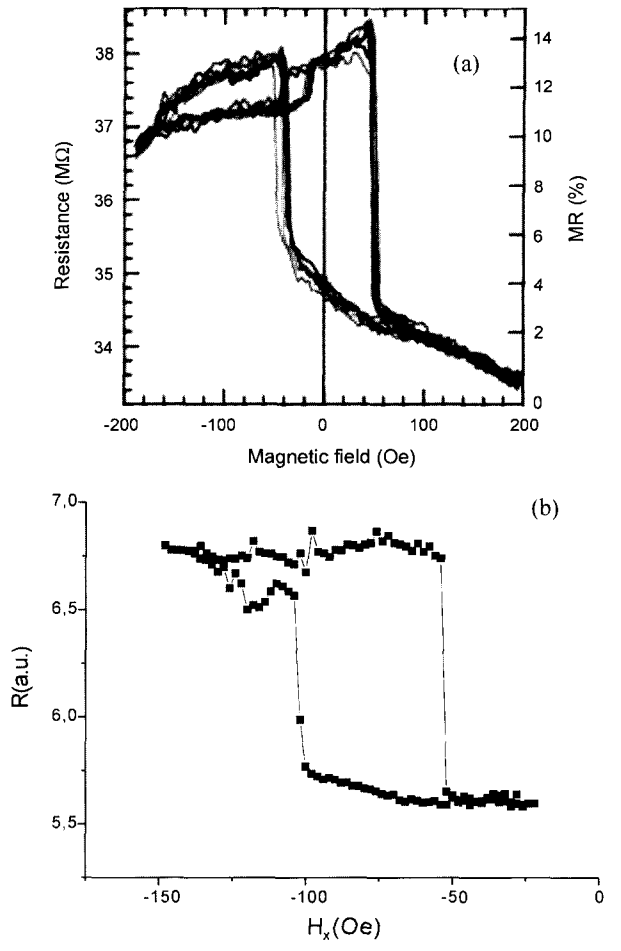

Fig. 4. TMR minor loops detected with a conducting tip AFM. The element size is 100 nm × 300 nm (a) and 50 nm × 50 nm (b).

to this finding, the smallest cells usually do not show any signs of domain splitting; for these junctions, we usually find nice minor loops with a large remanent magnetization and steep switching.

As can be additionally recognized in Fig. 4b, however, the minor loop is shifted by 75 Oe in the direction of the negative field, which in this case means an antiparallel coupling of the soft electrode to the hard layer system. The reason for this effect is a magnetic edge coupling effect illustrated in Fig. 5. A simple magnetostatic calculation gives an estimate of this coupling:

$$H_S = \frac{2M_s t W}{\pi(L^2 + 4x^2)\sqrt{1 + \frac{W^2 + 4x^2}{L^2}}} - H_N \qquad (2)$$

where M_s is the magnetization of the hard layer, t the thickness, W the width and L the length, respectively; x represents the thickness of the spacer layer and H_N the (in

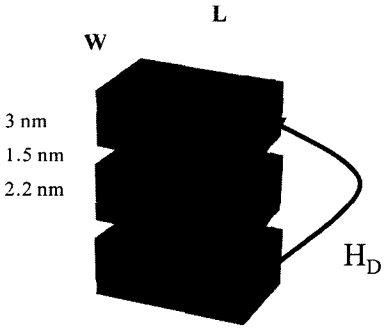

Fig. 5. Sketch of the effect of antiferromagnetic coupling of the ferromagnetic electrodes of a TMR junction by edge stray fields. The thicknesses given on the left are values typical for our tunneling junctions.

most cases ferromagnetic) coupling contribution of the orange peel effect.

Although this antiparallel coupling becomes very strong for small junctions, its strength can be reduced by the artificial antiferromagnet. In this case, the product $M_s t$ must be replaced by $(M^1{}_s t^1 - M^2{}_s t^2)$ for the two ferromagnetic layers 1 and 2. Therefore it should be even possible to compensate also the orange peel coupling by choosing appropriate materials and thicknesses. For small elements, the minor loops obtainable therefore are very promising for application.

Clearly, in the range of some hundreds of nm (Fig. 4a), problems occur due to magnetization reversal of single domains visible as jumps in the TMR curve, to vortex formation and to magnetization ripple in the hard layer leading to a non saturated TMR curve at the closure of the soft layer's hysteresis. These facts actually make TMR junctions biased simply by an af-coupled trilayer not suitable for application. For additional biasing by an natural antiferromagnet, however, still domain switching can be observed. This depends strongly on the shape of the element. In order to obtain more information, we therefore measured complete asteroid-curves. Some examples are shown in Fig. 6 for a trapezoidal junction 200 nm × 400 nm in size (a: measurement, b: simulation) and for a truncated elliptical junction 200 nm × 200 nm (c: measurement). Clearly, the latter one has an asteroid very suitable for double pulse switching. Here, the truncated elliptical shape favors a C-state as remanent magnetization configuration and suppresses vortices and 360° domain walls. Thus it seems to be possible to obtain suitable tunneling elements also in this size range by tailoring the shape and thereby the anisotropy.

3.2. Applications–TMR

As demonstrated, the TMR cells promise to be operable down to sizes of 200 nm × 200 nm and much smaller;

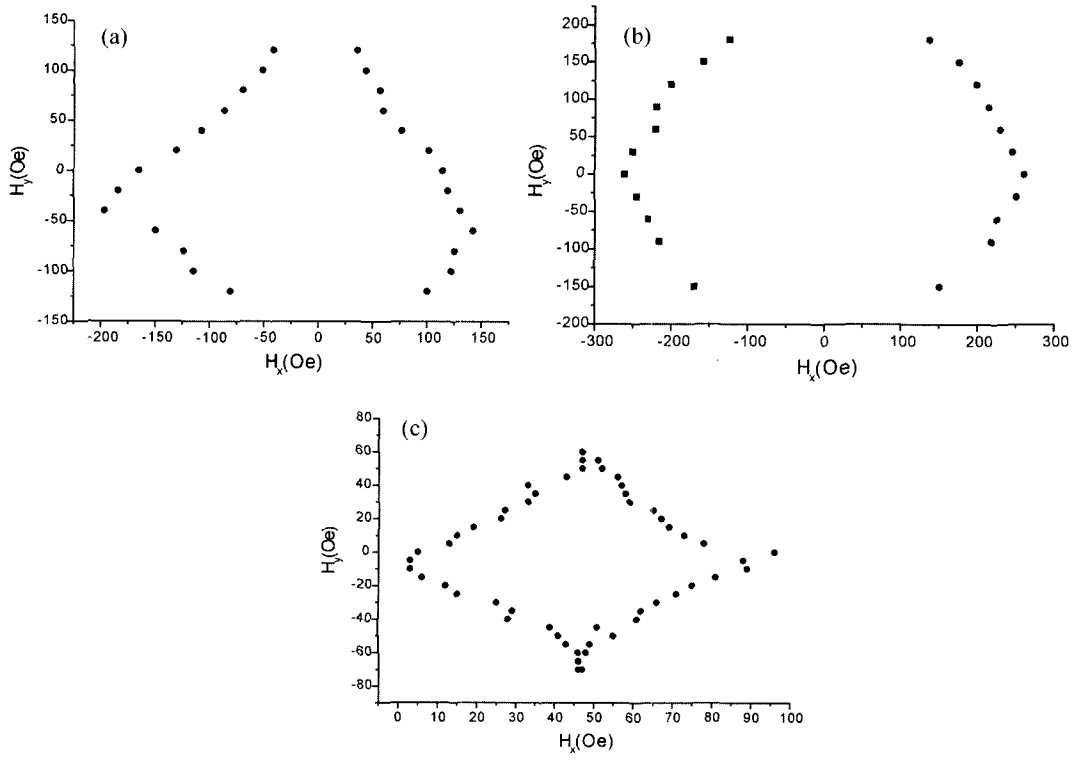

Fig. 6. Asteroid curves taken with the c-AFM for a trapezoidal junction 200 nm × 400 nm (a: measurement, b: simulation) and for a truncated elliptical junction 200 nm × 200 nm (c: measurement).

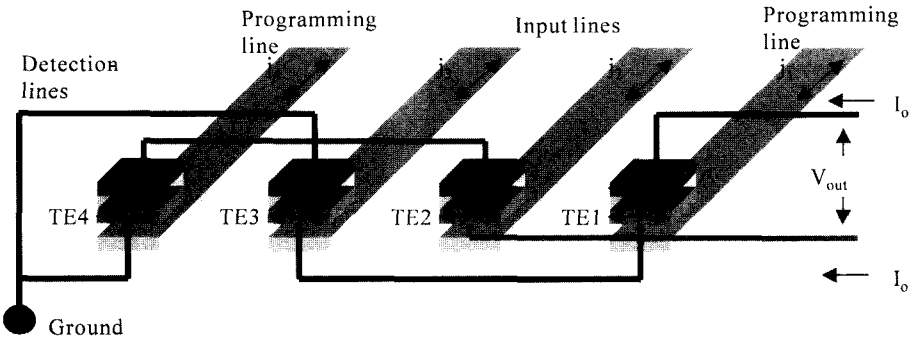

Fig. 7. Sketch of a logic gate array of TMR elements (TE1-TE4). The current I_o through all tunneling elements has the same value, TE 1 and 3 and TE 2 and 4 are switched in series, respectively. The output is the voltage V_{out}.

thus many of the main requirements on TMR systems for the use in MRAMís seem to be fulfilled. Although there are surely still a lot of technical and cost problems to be solved, we will concentrate here on some 'non-traditional' applications, which may become important beyond MRAM.

Magnetic logic

Magnetic logic means to create logic gates which are compatible with MRAM and are able to perform logic operations such as AND, NOR or NAND. First steps have been published by the group of Cowburn using magnetic patterns and moving therein domain walls [20]. Our approach [9] uses the tunneling cells discussed in the foregoing sections within a bridge-arrangement (Fig. 7).

Here, the same current I_o runs through the tunneling elements, whereby TE 1 and 3 and TE 2 and TE 4 are switched in series, respectively. The soft electrodes are magnetically switched by running currents through the input or the programming lines. Thus, logic input 1 means, *e.g.*, current running through one of the input lines and switching either element 2 or 3 in fig. 7. The output is represented by the voltage V_{out}, where a voltage larger than a certain value $U_{gap,\ top}$ means logic 1 and smaller than another $U_{gap,\ bottom}$ means logic 0. These two regions must be separated by a gap of at least 30 mV-40 mV, *i.e.* $(U_{gap,\ top}-U_{gap,\ bottom}) > 40$ mV, in order to reliably distinguish the two possible output signals.

The output signal itself is defined by the resistance states of all elements, *i.e.* both the input elements TE 2 and TE 3 as well as the 'program-elements' TE 1 and TE 4 in Fig. 7. Thus this logic gate can be programmed by magnetically switching these latter tunneling junctions and thereby changing their resistance state. Although a similar programmable operation is already available with standard semiconductor devices, this approach gives a much faster and less power consuming operation, opening the fascinating field of reconfigurable computing for magnetoelectronics. For computing, however, a clocked operation is necessary. This can be obtained by an additional current line (not shown in Fig. 7) supplying a clock-field which points to the hard axis direction of the tunneling elements. Thus magnetic switching will only occur if both the hard axis clock field and the soft axis input or the programming field is present.

In Fig. 8, we show the result of operating a 6-element logic gate in an AND configuration with clocked operation. The upper part shows the time evolution of clock, input, electronically treated and original output signals and the corresponding magnetic configuration of the elements.

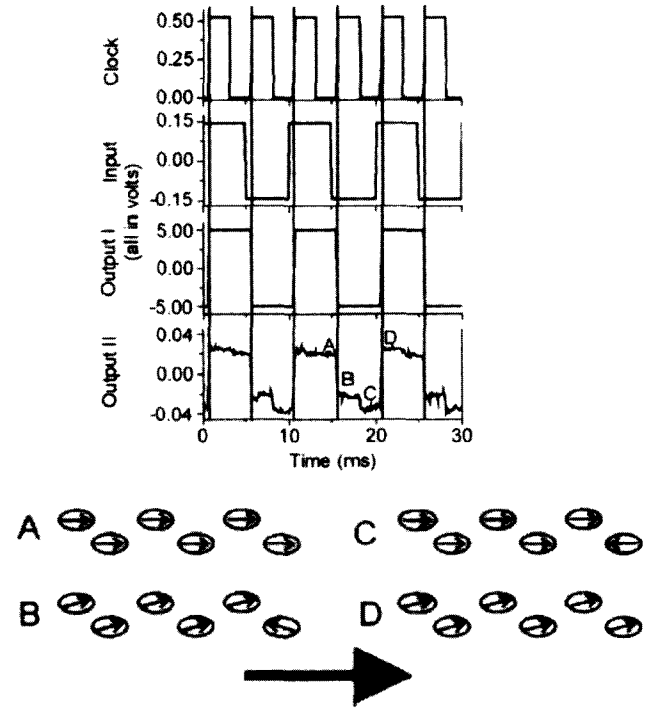

Fig. 8. Clocked operation of a 6-element logic gate in an AND configuration. Clock signal (top, hard axis field), input (easy axis field), electronically treated (output I) and original output (output II). The lower sketch shows the corresponding magnetization states.

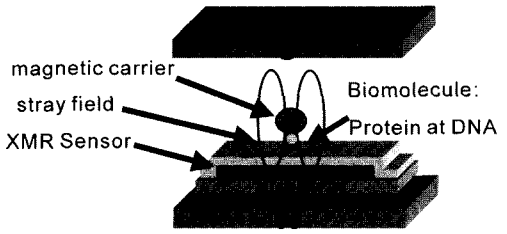

Fig. 9. Sketch of the detection of magnetic particles attached to molecules with an XMR-sensor. There is no direct response to the perpendicular field; the induced dipole field of the beads generates in plane components which produce a resistance change.

Clearly, a truly clocked operation as well as a voltage gap of the two output values larger than 40 mV can be obtained. Thus this can be regarded as a proof of principle for this kind of field programmable logic device.

There are, however, still efforts to be done, because the requirements for logic are much more stringent than for MRAM: Both the TMR as well as the resistance of all cells have to match extremely well. Although this can be usually obtained for the TMR, the resistance remains a problem due to its exponential dependence on the barrier thickness and height. Work going on on this topic, however, shows quite promising results.

Biological and applications in genetics

Although it may sound a little bit strange, both GMR and TMR elements could also be used to detect biological molecules as DNA or proteins [10]. The molecules are attached to small magnetic markers or carriers (usually called beads), which are commercially available already functionalized to form, *e.g.*, biotin-streptavidin bonds. These molecules are given in a fluid and swept over the protected surface of an XMR (*i.e.* GMR or TMR) sensor.

If now the surface of the protection layer is already functionalized with, *e.g.*, complimentary DNA strands, specific binding of the biomolecules will occur. Magnetically, there will be a bead present if binding occurs and no bead vice versa.

The detection of these beads now is done by applying a field perpendicular to the plane of the sensor (Fig. 9). Due to its large in plane anisotropy, there will be no direct response to this field; in the presence of beads, however, their induced dipole field generates in plane components in the sensor, which gives rise to a resistance change.

In Fig. 10, we show the results of this measurements. On the left side, a SEM image of the bead covered surface of a protected TMR sensor is shown. The graph on the right gives the resistance response as a function of the external perpendicular field for different amounts of bead coverage. Careful evaluation of these measurements show a linear response of the resistance for a bead coverage between about 3% and around 50% of the total surface area. Moreover, the large sensitivity of the TMR elements should allow for even single bead und thus single molecule detection.

Together with the possibility to manipulate such beads by magnetic field generated on the chip, this could also enable us to measure forces between individual molecules.

4. Conclusions

Following the discovery of Peter Grünberg, a large number of basic research and closely related applications were and still are launched within extremely short time, all summarized as 'Magnetoelectronics' or 'Spinelectronics'.

Researchers tried to understand the basic principles of spin dependent transport and tunneling. At the same time, applications as sensors and / or storage devices are already established or currently emerging, which offer large signal to noise ratios and have the potential of

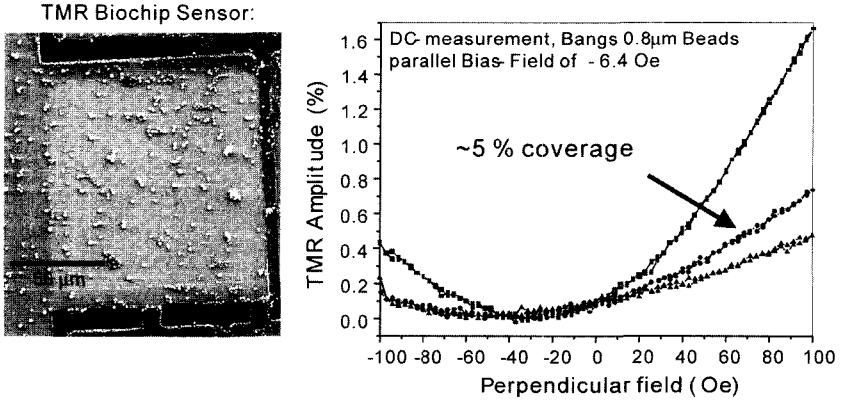

Fig. 10. SEM image of the bead covered surface of a TMR sensor (a) and the resistance response as a function of the external perpendicular field for different amounts of bead coverage (b).

overcoming the volatility of information storage and the current limits of integration density.

A considerable number of the demands, MRAM puts on magnetic tunneling elements, either are already met or seem to be at least no major obstacles. Research further demonstrates possibilities beyond the presently anticipated MRAM, especially in the fields downscaling, of logic and biochips.

Moreover, the recent discovery of magnetoelectronic effects in semiconductors opens the additional field of optoelectronics. Thus a rapid growth of possible applications seems to be still ahead, opening the final goal of fully integrated 'Spintronics'.

References

[1] P. Grünberg, R. Schreiber, Y. Pang, M. B. Brodsky, and H. Sowers, Phys. Rev. Lett. **57**, 2442 (1986).

[2] J. S. Moodera, L. R. Kinder, T. M. Wong, and R. Meservey, Phys. Rev. Lett. **74**, 3273 (1995).

[3] T. Miyazaki and N. Tezuka, J. Magn. Magn. Mater. **139**, 231 (1995).

[4] J. S. Moodera, L. R. Kinder, T. M. Wong, and R. Meservey, Phys. Rev. Lett. **74**, 3273 (1995).

[5] S. S. P. Parkin, K. P. Roche, M. G. Samant, P. M. Rice, R. B. Beyers, R. E. Scheuerlein, E. J. O'Sullivan, S. L. Brown, J. Bucchigano, D. W. Abraham, Y. Lu, M. Rooks, P. L. Trouilloud, R. A. Wanner, and W. J. Gallagher, J. Appl. Phys. **85**, 5828 (1999).

[6] R. C. Sousa, J. J. Sun, V. Soares, P. P. Freitas, A. Kling, M. F. da Silva, and J. C. Soares, Appl. Phys. Lett. **73**, 3288 (1998).

[7] M. Sato, H. Kikuchi, and K. Kobayashi, J. Appl. Phys. **83**, 6691 (1998).

[8] J. Schmalhorst, H. Brückl, G. Reiss, G. Gieres, M. Vieth, and J. Wecker, J. Appl. Phys. **87**, 5191 (2000).

[9] R. Richter, L. Bär, J. Wecker, and G. Reiss, Appl. Phys. Lett. **80**, 1291 (2002).

[10] J. Schotter, P. B. Kamp, A. Becker, A. Pühler, D. Brinkmann, W. Schepper, H. Brückl, and G. Reiss, A Biochip based on Magnetoresistive Sensors, IEEE Trans. Magnet., accepted.

[11] A. M. Bratkovsky, Phys. Rev. B **56**, 2344 (1997).

[12] M. Tsunoda, K. Nishikawa, S. Ogata, and M. Takahashi, Appl. Phys. Lett. **80**, 3135 (2002).

[13] S. Gider, B.-U. Runge, A. C. Marley, and S. S. P. Parkin, Science **281**, 797 (1998).

[14] L. Thomas, J. Lüning, A. Scholl, F. Nolting, S. Anders, J. Stöhr, and S. S. P. Parkin, Phys. Rev. Lett. **84**, 3462 (2000).

[15] M. R. McCartney, R. E. Dunin-Borkowski, M. R. Scheinfein, D. J. Smith, S. Gider, and S. S. P. Parkin, Science **286**, 1337 (1999).

[16] H. A. M. van den Berg, W. Clemens, G. Gieres, G. Rupp, M. Vieth, J. Wecker, and S. Zoll, J. Magn. Magn. Mater. **165**, 524 (1997).

[17] H. Brückl, J. Schmalhorst, H. Boeve, G. Gieres, and J. Wecker, J. Appl. Phys. **91**, 7029 (2002).

[18] D. Meyners, H. Brückl, and G. Reiss, Influence of boundary roughness on magnetization reversal in submicron sized magnetic tunnel junctions, J. Appl. Phys., accepted.

[19] H. Kubota, G. Reiss, H. Brückl, W.Schepper, J. Wecker, and G. Gieres, Jap. J. Appl. Phys. **41**, L180 (2002).

[20] D. A. Allwood, G. Xiong, M. D. Cooke, C. C. Faulkner, D. Atkinson, V. Vernier, and R. P. Cowburn, Science **296**, 5575 (2002).